

OPEN

Fucosylated inhibitors of recently identified bangle lectin from *Photorhabdus asymbiotica*

Gita Paulíková^{1,2}, Josef Houser^{1,2}, Martina Kašáková³, Beáta Oroszová³, Benedetta Bertolotti³, Kamil Parkan³, Jitka Moravcová³ & Michaela Wimmerová^{1,2,4*}

A recently described bangle lectin (PHL) from the bacterium *Photorhabdus asymbiotica* was identified as a mainly fucose-binding protein that could play an important role in the host-pathogen interaction and in the modulation of host immune response. Structural studies showed that PHL is a homo-dimer that contains up to seven L-fucose-specific binding sites per monomer. For these reasons, potential ligands of the PHL lectin: α -L-fucopyranosyl-containing mono-, di-, tetra-, hexa- and dodecavalent ligands were tested. Two types of polyvalent structures were investigated – calix[4]arenes and dendrimers. The shared feature of all these structures was a C-glycosidic bond instead of the more common but physiologically unstable O-glycosidic bond. The inhibition potential of the tested structures was assessed using different techniques – hemagglutination, surface plasmon resonance, isothermal titration calorimetry, and cell cross-linking. All the ligands proved to be better than free L-fucose. The most active hexavalent dendrimer exhibited affinity three orders of magnitude higher than that of standard L-fucose. To determine the binding mode of some ligands, crystal complex PHL/fucosides 2 – 4 were prepared and studied using X-ray crystallography. The electron density in complexes proved the presence of the compounds in 6 out of 7 fucose-binding sites.

Reversible interactions between the oligosaccharide chain of glycolipids/glycoproteins and carbohydrate-binding protein receptors (lectins) mediate critical biological recognition at the cell level. They are of vital importance in many normal and pathological processes ranging from fertilization, immune response and intercellular communication to viral/bacterial invasion and tumour metastasis¹. The identification of lectin-carbohydrate interactions in human diseases raises the possibility of the development of carbohydrate-based therapeutic products. Anti-adhesion therapy has been used for a few decades and the protective effect of anti-adhesive saccharides has been demonstrated in several studies². For example, mannose has been used to treat urinary tract infections caused by *E. coli*. Moreover, the anti-adhesive agents do not kill pathogens or arrest their growth thus development of resistance to anti-adhesive agents will be less likely as compared to antibiotics^{2,3}. Therefore, anti-adhesion therapy is a very attractive approach that not only prevents infections at an early stage but is also an important alternative treatment for bacterial infection considering the alarming increase of drug-resistant bacteria.

P. asymbiotica was originally considered to be exclusively an insect pathogen until 1989, when it was isolated from a patient in the USA for the first time⁴. Later on, further human infections were reported in Australia⁵ and nowadays, occurrence of this bacterium is not restricted to American and Australian continents but starts to be globally spread^{6–10}. *P. asymbiotica* is regarded as an emerging human pathogen causing either locally invasive or disseminated soft-tissue infections^{11–14}. Relatively low number of infections has been reported so far, however this is likely to be caused by misidentification by automated microbiological techniques, which do not contain *Photorhabdus* sp. in their databases¹². Recently, the two subspecies of *P. asymbiotica* (*P. asymbiotica* subsp. *asymbiotica* and *P. asymbiotica* subsp. *australis*) were suggested to be elevated into a higher taxon, creating the *P. asymbiotica* and *P. australis* species, respectively¹⁵.

As a part of our ongoing programme focused on host-pathogen interactions at the molecular level, we identified a lectin in the *P. asymbiotica* genome designated PHL, which we prepared in a fully functional recombinant form¹⁶. We also determined its carbohydrate specificity and investigated the structural details of ligand binding.

¹Central European Institute of Technology, Masaryk University, Brno, Czech Republic. ²National Centre for Biomolecular Research, Faculty of Science, Masaryk University, Brno, Czech Republic. ³Department of Chemistry of Natural Compounds, University of Chemistry and Technology, Prague, Czech Republic. ⁴Department of Biochemistry, Faculty of Science, Masaryk University, Brno, Czech Republic. *email: michaw@chemi.muni.cz

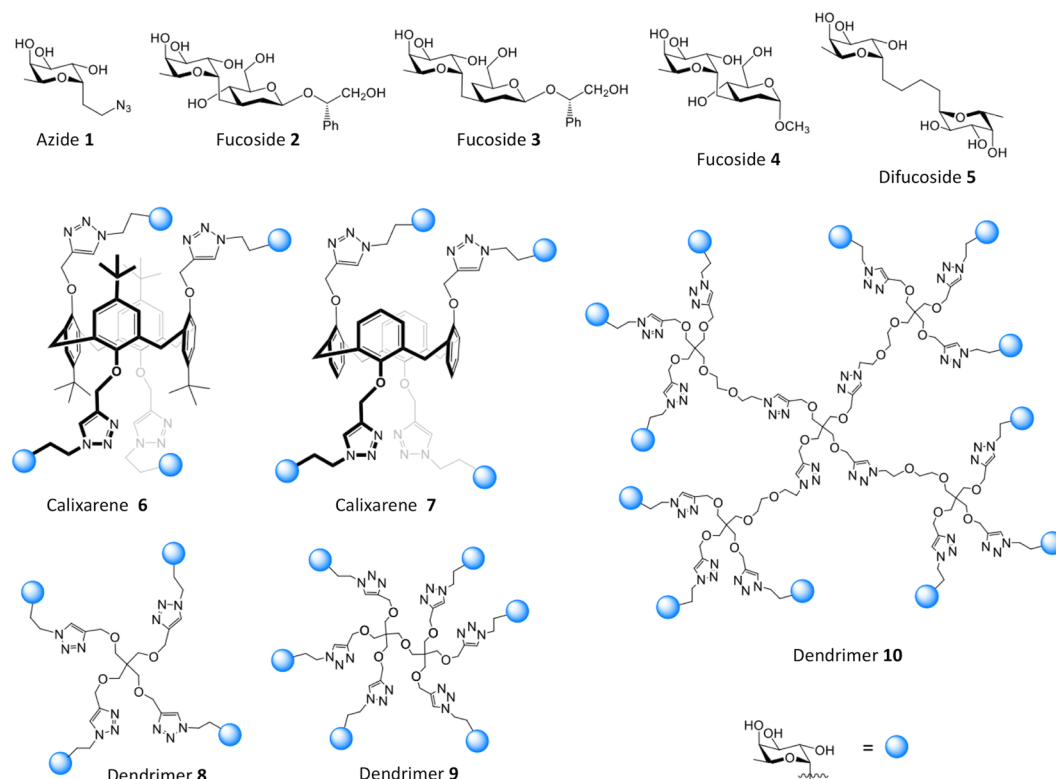


Figure 1. Structure of ten tested α -L-fucopyranosyl compounds.

Moreover, PHL demonstrated the ability to act as a host-cell recognizing agent through interacting with the haemolymph of *Galleria mellonella* (order Lepidoptera, family Pyralidae) and human blood components and also to modulate immune system of both hosts¹⁶. Lectins of other bacteria were confirmed as virulence factors, e.g. PA-IL and PA-IIL from opportunistic *Pseudomonas aeruginosa* or FimH from uropathogenic *Escherichia coli* (UPEC) strains^{17,18}. The PHL lectin can play equally important role as above-mentioned examples and therefore, PHL could be a usable therapeutic target. Interestingly, other two saccharide-binding proteins were detected in *Photobacterium* genus – PLL and PIIA, both from *P. luminescens*^{19,20}. PLL is a fucose-specific lectin and a sequence homologue of PHL. However, PLL is not able to modulate the host innate immune response as PHL and probably plays a role in bacteria-nematode interactions. The PIIA lectin is a galactose-specific lectin and homologue of PA-IL (LecA) from *Pseudomonas aeruginosa*, which is known for its utilization in *P. aeruginosa* infection and biofilm formation in lung of patients with cystic fibrosis²¹. Due to the PIIA specificity, the certain role both in the symbiosis with their nematode hosts and in insect infection is speculated.

The lectin PHL interacts selectively, mainly with L-fucose and oligosaccharides containing terminal L-fucose residue, and prefers an α -glycosidic bond over a β -linkage. Surface plasmon resonance (SPR) in a competition assay revealed that methyl α -L-fucopyranoside, with an IC_{50} of 40 μ M, was about a 10-fold stronger ligand than free L-fucose. Nevertheless, the IC_{50} value is in the low μ M range, suggesting a relatively weak binding of methyl α -L-fucopyranoside to PHL. The preparation of a core L-fucose derivative bearing suitable functional groups for the construction of multivalent systems could enhance this affinity substantially.

Here we present a comprehensive study covering interactions of the lectin PHL with a pool of L-fucose-based potential ligands with different valences and topologies, assessed by hemagglutination, SPR, isothermal titration calorimetry (ITC), and cell cross-linking assays. All constructs are stable against both acidic and enzymatic hydrolysis due to the presence of C-glycosidic bonds. In most of the experiments, dendrimers emerged as the best ligands, especially the hexafucosylated dendrimer 9. During SPR measurement, dendrimer 9 had a potency per fucose unit that was over 1,600 times as effective as L-fucose and 52 times as respective saccharide-building unit azide 1. The structure of PHL complexes with fucosides 2–4 was solved using X-ray crystallography, and compounds were found in 6 out of 7 fucose-binding sites of at least one PHL monomer unit.

Result and Discussion

Ligands tested. In total 10 compounds with α -L-fucopyranosyl unit(s) were selected from our library of recently synthesized potential ligands towards various lectins (Fig. 1). Azide 1²² is an analogue of methyl α -L-fucopyranoside, and also serves for the preparation of polyvalent systems. The previous study showed increased affinity to di- and tri-saccharides for PHL. Therefore, pseudo-C-disaccharides 2–4²³ as monovalent ligands differing in the structure of the C-aglycone part were included in the study to analyse the potential influence of the second saccharide-like unit on the ligand binding. 1,4-bis(fucopyranosyl)butane 5²³ is a divalent mimetic in which the distance between the C1 atoms of both α -L-fucopyranosyl units is derived from the structure of blood group

Ligand	Valency	MIC [μM]	Potency _{L-Fuc}	$\beta_{\text{L-Fuc}}$	Potency _{Azide1}	β_{Azide1}
Fucoside 2	1	6,400	0.5	0.5		
l-Fuc	1	3,200	1	1		
Fucoside 4	1	1,600	2.0	2.0		
Fucoside 3	1	500	6.4	6.4		
α -Me-Fuc	1	400	7.8	7.8		
Azide 1	1	200	15.6	15.6	1	1
Difucoside 5	2	200	15.6	7.8		
Calixarene 6	4	100	31.3	7.8	2	0.5
Calixarene 7	4	100	31.3	7.8	2	0.5
Dendrimer 8	4	50	62.5	15.6	4	1
Dendrimer 9	6	25	125	20.8	8	1.3
Dendrimer 10	12	25	125	10.4	8	0.7

Table 1. Hemagglutination inhibition assay with PHL. Minimal inhibitory concentrations (MIC) of synthesised inhibitors and their potency towards L-fucose were determined using two independent measurements. To assess the contribution of valency to the MIC, an affinity improvement factor β was calculated as the relationship $\text{MIC}_{\text{basic unit}}/(\text{valency} \times \text{MIC}_{\text{ligand}})$.

Lewis b tetrasaccharide. Tetravalent constructs **6** and **7** contain a calix[4]arene scaffold in a 1,3-*alternate* conformation that ensures sufficient solubility in water. Both **6** and **7**²⁴ were prepared by CuAAC click reaction^{25,26} from azide **1** and the respective tetrapropargyl calix[4]arene. Finally, a set of dendrimers **8–10**²² with valences ranging from 4 to 12 are more flexible and complex ligands than calix[4]arene derivatives, thus a significant increase in the complexity of the binding event can be expected. The affinity improvements in multivalent carbohydrate–lectin interactions have been attributed to the so-called “cluster glycoside effect”^{27–29}.

Hemagglutination inhibition assay. PHL as a fucose-specific lectin was shown to agglutinate papain-treated RBCs of blood group O¹⁶ with the surface-exposed terminal trisaccharide α -L-Fucp-(1 \rightarrow 2)- β -D-Galp-(1 \rightarrow 3/4)-D-GlcpNAc. The set of potential ligands **1–10** with different levels of fucosylation was tested, and their inhibition potency on hemagglutination by PHL was assessed (Table 1, Fig. 2). DMSO-containing blank did not affect the hemagglutination in any way. To assess the contribution of valency to the affinity increase, an affinity improvement factor β was calculated as the relationship $\text{MIC}_{\text{basic unit}}/(\text{valency} \times \text{MIC}_{\text{ligand}})$.

Simple monovalent fucosides **2–4** failed to substantially inhibit the hemagglutination caused by PHL, while azide **1** and difucoside **5** were 16-fold better inhibitors than L-fucose and twice as good as methyl α -L-fucopyranoside. If the structures of simple ligands **1–5** are compared, it seems that the nonpolar substituent at the anomeric position of L-fucose provides an advantage. The activities of tetravalent calixarenes **6** and **7** are identical, giving a potency of 31.3 without regard to the presence or absence of a *tert*-butyl group on the upper rim of the skeleton. Tetravalent dendrimer **8** was as efficient inhibitor of hemagglutination as calixarenes **6** and **7**, although it occupies a different topology. Hexa- and dodeca-fucosylated dendrimers **9** and **10** were proven to be the best inhibitors. They were more than 100-fold better ligands than natural L-fucose. However, according to the β factor calculated with respect to azide **1** (β_{Azide1}), all multivalent compounds were comparable with their building unit.

Surface plasmon resonance. To analyse the competitive inhibition of PHL binding to a multivalent surface, the surface plasmon resonance (SPR) technique was employed. A sensor chip presenting α -L-fucopyranoside residues was treated with a constant concentration of PHL, while an increasing concentration of the ligands was used to determine IC₅₀ (Table 2, Fig. 3). Only the ligands comparable with or better than α -Me-Fuc in the hemagglutination assay were investigated by SPR. To assess the contribution of valency to the affinity increase, an affinity improvement factor β was calculated as the relationship $\text{IC}_{50, \text{basic unit}}/(\text{valency} \times \text{IC}_{50, \text{ligand}})$ ³⁰.

Comparing the IC₅₀ values and potency, the results from SPR are in good agreement with the finding obtained by hemagglutination. Azide **1** and fucoside **3** exhibit 32-fold and 38-fold, respectively, stronger affinity to PHL than its counterpart L-fucose; in fact, an 86-fold increase in affinity was found for difucoside **5**. The affinity improvement factors of tetravalent calixarenes **6** and **7** as well as dendrimer **8** were comparable with β_{Azide1} value reaching approximately 15. The hexavalent dendrimer **9** was the best ligand of the lectin PHL with IC₅₀ = 37 nM, β_{Azide1} = 52 and with potency 9,800-fold and 310-fold higher than L-fucose and azide **1**, respectively. Although dodecavalent dendrimer **10** was also an efficient ligand (IC₅₀ = 80 nM), its affinity improvement factor was substantially lower (β_{Azide1} = 12) than that of the hexavalent dendrimer **9**. This observation could be caused by unwanted side effects such as cross-linking or aggregation induced by the sterically demanding structure of **10**. Nevertheless, the data support a strong glycoside clustering effect.

Isothermal titration calorimetry. The binding of PHL to different α -L-fucoside compounds was further characterized by isothermal titration calorimetry (ITC), enabling determination of the complete thermodynamic profile of the molecular interactions (Table 3, Fig. 4). As for calixarenes, both compounds caused a cross-linking/aggregation of PHL accompanied by the formation of visible precipitates. Because of this, it was not possible to evaluate the data, despite the obvious interaction. The dendrimers also cross-linked/aggregated the protein

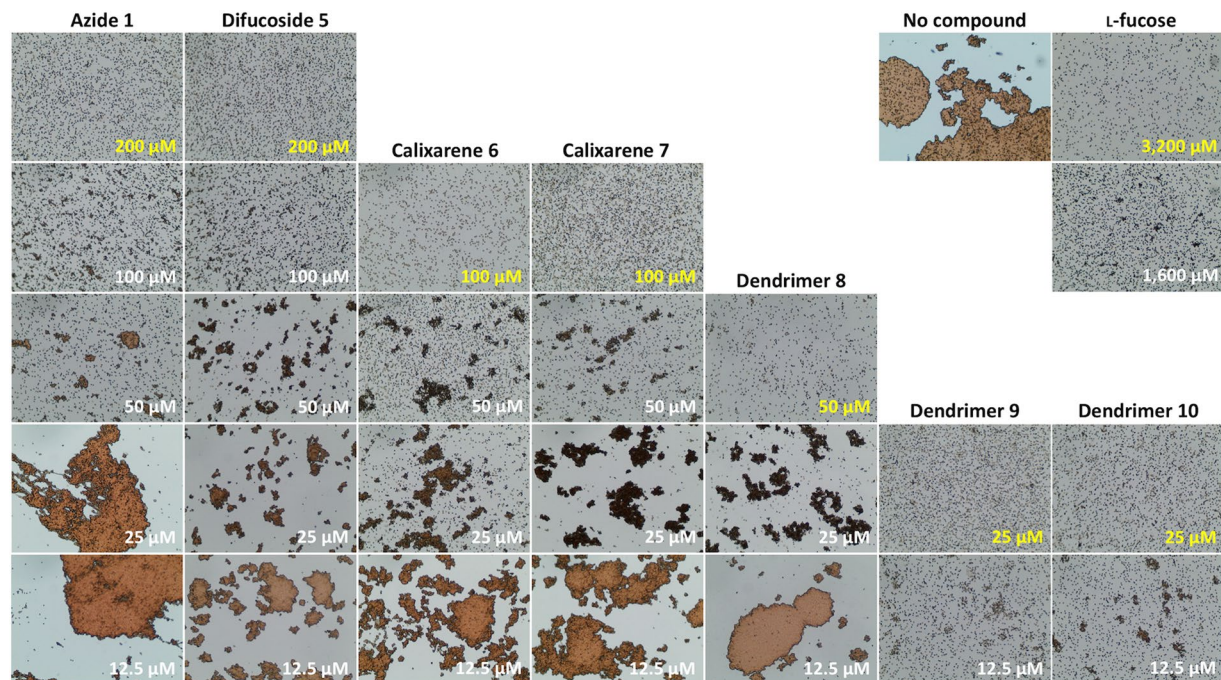


Figure 2. Representatives of α -L-fucopyranosyl compounds with a higher potency than α -Me-Fuc and their influence on hemagglutination of RBC O caused by PHL. Two-fold serially diluted carbohydrate compounds **1**, **5–10** were able to inhibit hemagglutination at the minimal concentrations highlighted in yellow. The hemagglutination of RBC O caused by PHL without an inhibitor is shown in the picture in the upper right corner.

Ligand	Valency	IC ₅₀ [μ M]	Potency _{L-Fuc}	β_{L-Fuc}	Potency _{Azide1}	β_{Azide1}
L-Fuc	1	362 \pm 33	1	1		
α -Me-Fuc	1	38.5 \pm 1.2	9	9		
Fucoside 3	1	12.9 \pm 0.6	28	28		
Azide 1	1	11.5 \pm 1.4	32	32	1	1
Difucoside 5	2	4.18 \pm 0.42	86	43		
Calixarene 6	4	0.195 \pm 0.023	1,853	464	59	15
Dendrimer 8	4	0.188 \pm 0.037	1,922	481	65	16
Calixarene 7	4	0.178 \pm 0.020	2,029	508	61	15
Dendrimer 10	12	0.080 \pm 0.011	4,538	377	144	12
Dendrimer 9	6	0.037 \pm 0.003	9,762	1,631	311	52

Table 2. Inhibition activity of studied ligands towards PHL assessed by SPR. IC₅₀ was determined from three independent measurements. To assess the contribution of valency to the IC₅₀, an affinity improvement factor β was calculated as the relationship $IC_{50, \text{basic unit}} / (\text{valency} \times IC_{50, \text{ligand}})$.

as with calixarenes, however the curves provided clear outcomes with an affinity in the low micromolar range. The dissociation constants (K_D) of all dendrimers correlate with their valency – the higher number of fucose, the more decreased K_D . This implies that dodecafucoylated dendrimer **10** was assessed as the best inhibitor, with K_D almost 4 times better than the second-best hexavalent dendrimer **9** and 33 times better than azide **1** ($\beta_{Azide1} = 3$). The stoichiometry value n corresponds to the number of terminal fucoses per ligand molecule. The n value decreases from 4 to 1 as the number of fucose units increases from 1 to 12 (Table 3).

As for monovalent (azide **1**, fucoside **3**) and divalent (difucoside **5**) compounds, all of them exhibited a low affinity towards PHL (in the millimolar range), as is usually observed for lectin/saccharide interactions. They also correspond with the same β factor.

P. asymbiotica cross-linking – Bacterial aggregation properties. Because of the aggregation of PHL by calixarenes and dendrimers during SPR and ITC experiments, we decided to compare tetravalent compounds at a higher level. We performed a series of *in vitro* aggregation assays to reveal their aggregation properties towards *P. asymbiotica* subsp. *australis* (Table 4, Fig. 5). Prior to each assay, we confirmed the absence of aggregates in two negative controls – bacterial cells in PBS buffer and in the presence of azide **1** as a monomer. With all chosen compounds, we observed bacterial aggregates of a variable size that confirmed that they are capable

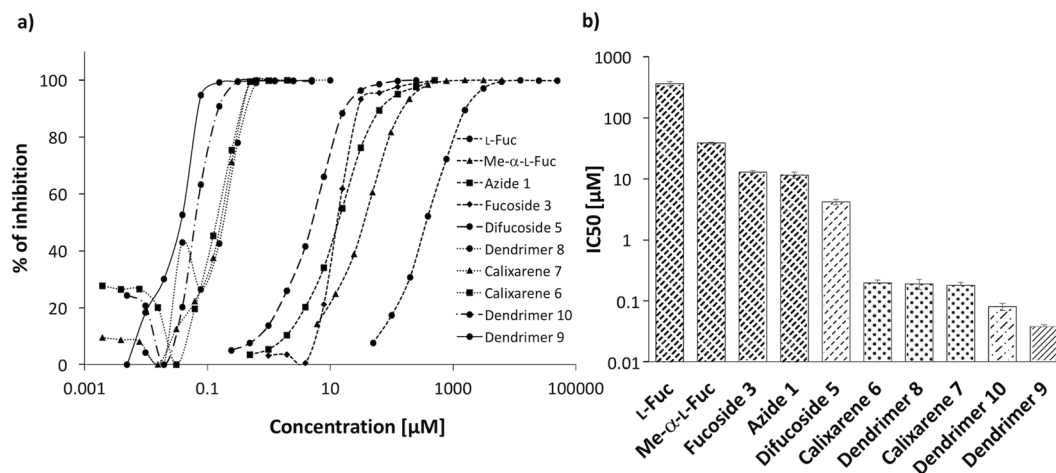


Figure 3. IC_{50} determination of fucoligands towards PHL from SPR measurements. **(a)** A logarithmic plot of inhibition curves calculated from SPR experiments vs. % of inhibition. Individual types of line correspond to monovalent (densely dashed), divalent (dashed), tetravalent (dotted), hexavalent (dash-dotted) and dodecaivalent (solid) ligands. **(b)** A logarithmic plot of IC_{50} determined for individual mono/multivalent ligands. Measurements were performed in triplicates and standard deviations were calculated. Individual types of line correspond to monovalent (densely dashed), divalent (dashed), tetravalent (dotted), hexavalent (dash-dotted) and dodecaivalent (solid) ligands.

Ligand	Valency	n	K_D [μ M]	$-\Delta H$ (kJ/mol)	$-T\Delta S$ (kJ/mol)	$-\Delta G$ (kJ/mol)	Potency L-Fuc	β_{L-Fuc}	Potency _{Azide1}	β_{Azide1}
l-Fuc	1	3*	$1,395 \pm 33$	59.5 ± 1.0	43.2 ± 1.0	16.3 ± 0.4	1	1		
α -Me-Fuc	1	2.9 ± 0.2	267 ± 11	59.0 ± 4.2	38.6 ± 4.3	20.4 ± 0.9	5	5		
Fucoside 3	1	5.4 ± 0.3	187 ± 16	30.3 ± 2.0	9.0 ± 2.6	21.3 ± 1.8	7	7		
Difucoside 5	2	3.9 ± 0.2	120 ± 11	37.5 ± 2.6	15.1 ± 3.3	22.4 ± 2.1	12	6		
Azide 1	1	4.1 ± 0.3	105 ± 9	42.9 ± 3.9	20.2 ± 4.4	22.7 ± 2.0	13	13	1	1
Dendrimer 8	4	3.0 ± 0.1	36.9 ± 3.7	53.8 ± 1.9	28.6 ± 3.2	25.3 ± 2.5	38	9	3	1
Dendrimer 9	6	2.0 ± 0.0	12.5 ± 0.6	71.5 ± 0.8	43.5 ± 1.6	28.0 ± 1.3	112	19	8	1
Dendrimer 10	12	1.2 ± 0.0	3.2 ± 0.6	112.6 ± 3.5	81.2 ± 7.2	31.4 ± 6.3	436	36	33	3

Table 3. Thermodynamic profiles for interaction between PHL and ligands determined by isothermal titration calorimetry at 25 °C. Thermodynamic parameters were calculated from two independent measurements. To assess the contribution of valency to the affinity increase, an affinity improvement factor β was calculated as the relationship $K_{D, \text{basic unit}} / (\text{valency} \times K_{D, \text{ligand}})$. *The stoichiometry value of L-fucose was fixed during the fitting procedure because of the low-affinity interaction that also causes that ΔH and ΔS values may suffer from higher inaccuracy. The value was based on the α -Me-Fuc measurement and on the X-ray crystal structure of the PHL/BGH complex.

of interacting with a cell surface. This effect may be caused by interaction of the multivalent inhibitors with PHL or other receptors. The concentration of the first appearance of aggregates varied according to the nature of the ligand used. The highest efficiency (0.625 mM) was observed for the tetravalent dendrimer 8, as we expected. Calixarene 6 proved to be only half as good as dendrimer 8, and aggregated cells at a concentration of 1.25 mM. An unexpected observation was that calixarene 7 had the lowest aggregation potential. In contrast to other techniques (hemagglutination, SPR and ITC), where calixarenes 6 and 7 provided similar results, during cross-linking experiments calixarene 7 was four times worse than calixarene 6. At the same time, both tetrameric calixarenes 6 and 7 are in a 1,3-*alternate* conformation with the two-faced presentation of the fucopyranosyl epitopes on opposite regions probably occupying a similar spatial orientation. The only difference is the *tert*-Bu group on the upper rim in calixarene 6, which might contribute to nonpolar interactions with whole *P. asymbiotica* cells.

X-ray structure of PHL/fucosides complex. The PHL lectin forms a seven-bladed β -propeller assembling into a homo-dimer. Both units contain two types of binding sites situated between the blades and have different amino acid compositions and binding preferences¹⁶. As mixing PHL with the branched compounds leads to protein precipitation and thus prevents co-crystallization, the direct study of complexes was not possible. Soaking ligand-free PHL crystals with a low concentration of individual branched compounds did not result in complex formation while soaking with their higher concentrations led to a crystal decomposition. Therefore, we soaked the PHL crystals with monomeric fucoside 2, 3 and 4, respectively. The structure of these complexes was determined using X-ray diffraction (Table 5).

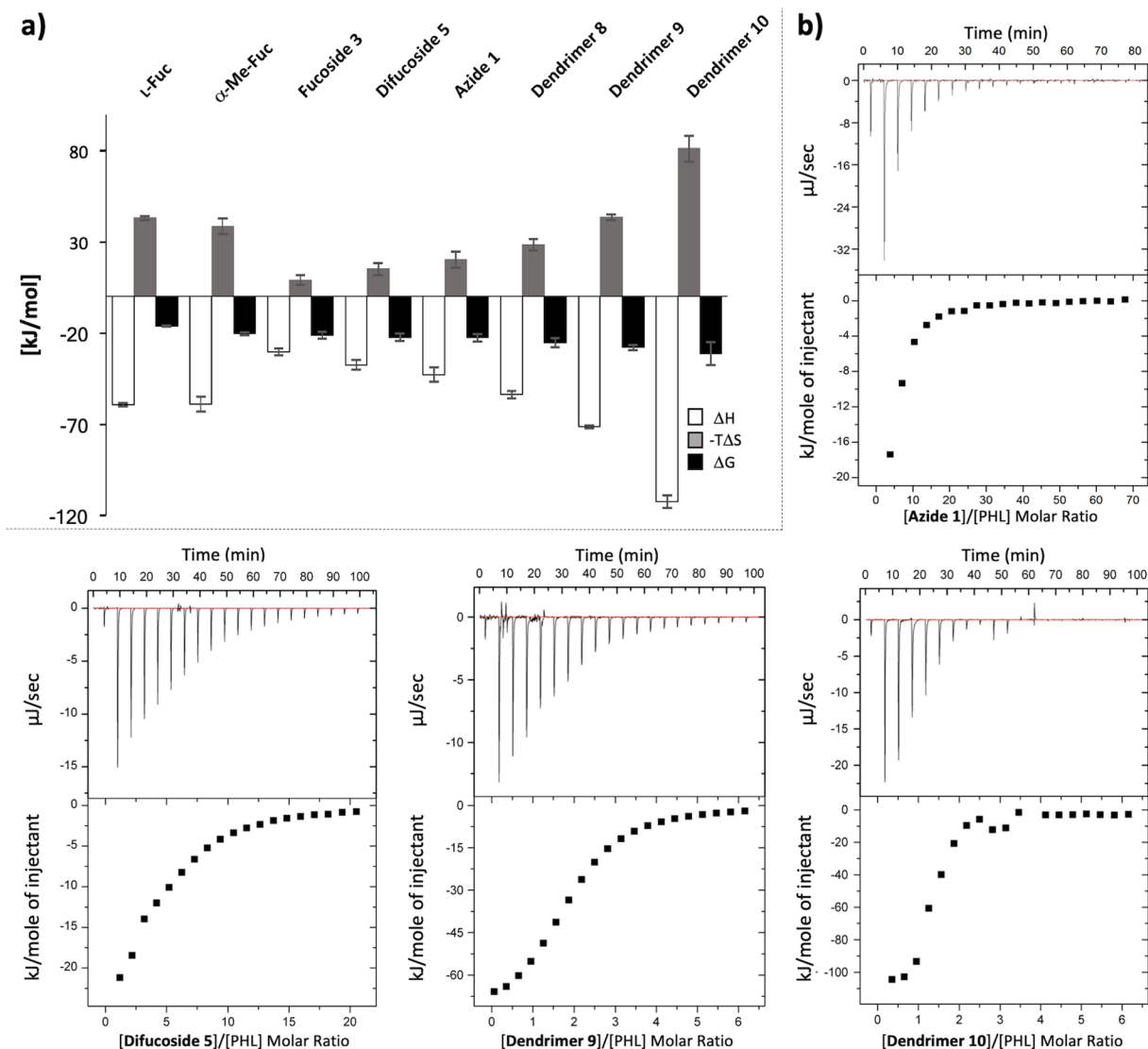


Figure 4. (a) Thermodynamic profiles for interaction between PHL and fucosyl ligands determined by isothermal titration calorimetry at 25 °C. (b) Selected ITC curves of PHL (50 μM) titration by azide 1 (5 mM), difucoside 5 (5 mM), dendrimer 9 (1.5 mM) and dendrimer 10 (1.5 mM). 20 injections of 2.0 μl of fucosyl clusters were added every 240 s to a PHL-containing cell. The lower plots show the total heat released as a function of total ligand concentration for the titration shown in the upper panels. Due to low affinity of PHL to monovalent compounds, n , ΔH and ΔS values may suffer from higher inaccuracy.

Ligand	Valency	The lowest concentration able to aggregate <i>P. asymbiotica</i> cells [mM]
Azide 1	1	No visible aggregation in used concentrations
Calixarene 7	4	5
Calixarene 6	4	1.25
Dendrimer 8	4	0.625

Table 4. Determination of minimal concentration of multivalent fucosyl clusters able to aggregate *P. asymbiotica* subsp. *australis* cells. Three independent measurements were performed.

Crystal structures confirmed that all the studied fucosides were able to bind the lectin PHL. In each complex, the electron density was clear enough to determine the position of the fucosyl part of the compounds in 6 out of 7 fucose-binding sites of at least one PHL monomer unit – A or B (Table 6, Fig. 6), while site 2 is occupied by Met60 of the neighbouring monomer, as was observed previously¹⁶. This demonstrates the binding potency of studied

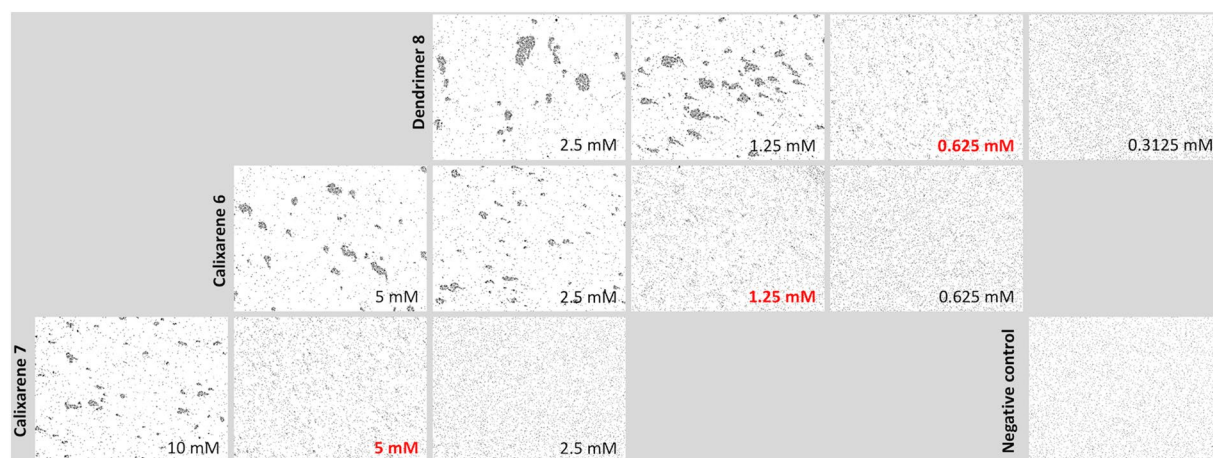


Figure 5. Representative images of optical microscopy observation (200x) of bacterial cell aggregation for *Photorhabdus asymbiotica* subsp. *australis* with different fucosylated clusters. Bacterial cells in PBS buffer were used as a negative control, shown in the bottom right image. Two-fold serially diluted carbohydrate compounds **6**, **7** and **8** were able to agglutinate the cells at minimal concentrations of 1.25 mM, 5 mM and 0.625 mM, respectively. The background of all pictures was subtracted in the software GIMP.

fucosides and experimentally confirmed a presence of at least 6 binding sites per monomer. In previous studies, only 2 to 5 binding sites were detected^{16,31}. The second saccharide unit was clearly assigned for all three fucosides **2–4** in sites 1 and 3. For fucoside **3** and **4**, the second saccharide was also distinguishable in sites 4–7 of at least one protein monomer (Table 6). This allows us to compare the binding mode for C-glycoside-based molecules and published previously O-glycoside structures. The fucose moiety is coordinated in the same way as was shown for α -Me-Fuc and blood group H trisaccharide¹⁶. Briefly, the O3, O4 and O5 of fucose are coordinated by the backbone atoms of two neighbouring loops and in sites 1, 3, and 5–7 also by the side chain of nearby threonine. The C6 methyl group and nonpolar surface of fucose are stabilized by a CH- π interaction with two tryptophan side chains. Considering fucosides **2–4**, the position of the bridging methylene group is close to the α -Me-Fuc O1 atom, which is not directly coordinated by the protein in the complex. Additional direct interactions between the protein and the studied molecules are infrequent. The O4 of the D-*arabino*-hexopyranosyl unit in fucoside **2** and **4** is coordinated by a glycine backbone nitrogen in sites 1, 3, 5, and 6, while the O6 atom of fucoside **3** is linked to a tryptophan backbone oxygen in sites 4 and 6. When comparing the overall orientation of the second hexopyranosyl unit of fucosides **2–4**, it is similar to the galactose unit of blood group H trisaccharide, with minor distortions in individual binding sites influenced e.g. by crystal packing. The remaining parts of fucosides **2** and **3** were not resolved in the electron density, suggesting their negligible importance for ligand binding.

Conclusions

In the previous study¹⁶, we identified an interesting lectin from emerging human pathogen *P. asymbiotica* harbouring seven potential fucose-binding sites per monomer and able to modulate innate immune system of human. Infection strategies used by pathogens often involve highly specific protein/carbohydrate interactions and therefore design of suitable inhibitors preventing this interaction is needed. Thus, we tested inhibition potency of L-fucose-based compounds with different valences and topologies. All these structures share the same feature of bearing C-glycosidic bond instead of the common but physiologically unstable O-glycosidic bond.

α -L-fucopyranosyl-containing mono-, di-, tetra-, hexa- and dodecavalent ligands were investigated by hemagglutination, ITC, SPR, X-ray crystallography, and cell cross-linking. The binding mode of monovalent ligands was studied via crystal complexes with PHL where the electron density proved the presence of the fucosyl part of the compounds in all accessible fucose-binding sites. The second saccharide unit of studied fucosides was only marginally coordinated by PHL binding sites what, together with affinity comparable to monosaccharides, suggests a low importance of this type of compounds for inhibitor design. On the other hand, the affinity towards azide **1** is thirteen times higher than towards L-fucose and comparable to previously studied propargyl- α -L-fucoside³¹. This suggests, together with data from the previously studied PHL complexes, that introduction of a linker with delocalized π -electrons has not negligible contributory effect to binding affinity and increases also binding site availability/occupancy (4–5 binding sites for azide **1**/propargyl- α -L-fucoside vs. 2–3 sites for α -Me-Fuc). This effect was already reported for the PA-III lectin and *p*-nitrophenyl- α -L-fucoside³². The affinity of PHL for multivalent ligands reached low micromolar values, which corresponds to an affinity three orders of magnitude higher than that of standard L-fucose and two orders of magnitude higher than that of monovalent azide **1**. We have further demonstrated that all of the tested compounds were able to inhibit the PHL binding towards both artificial and natural fucosylated surfaces. Generally, the potency of ligands depended on the valency and types of polyvalent structures (calix[4]arenes and dendrimers). Even though the relation between the increasing number of fucoses per cluster and increasing affinity, the most active compound was a hexavalent dendrimer exhibited an IC_{50} of 37 nM and K_D of 13 μ M. Several tetravalent compounds of different type were also tested for their ability to agglutinate *P. asymbiotica* bacteria. The cell clumps at different concentrations of tested compounds were observed

Molecule	PHL/fucoside 2	PHL/fucoside 3	PHL/fucoside 4
PDB ID	6FHX	6FHY	6FLU
Data collection			
Beamline	BESSY II 14.3	BESSY II 14.3	BESSY II 14.3
Wavelength (Å)	0.8943	0.8943	0.8943
Space group	P3 ₂ 21	P3 ₂ 21	P3 ₂ 21
Unit-cell parameters			
a and b (Å)	81.57	81.35	81.94
c (Å)	222.91	222.78	224.65
α = β [°]	90	90	90
γ [°]	120	120	120
Resolution range (Å)	44.58-2.34 (2.40-2.34)	44.56-1.86 (1.91-1.86)	44.93-1.78 (1.82-1.78)
Reflections measured	407636 (58160)	813765 (116126)	941162 (132122)
Unique reflections	37127 (5331)	73161 (10443)	85234 (12197)
Completeness (%)	99.9 (99.2)	99.9 (99.2)	100.0 (99.5)
CC1/2	99.2 (68.9)	99.6 (57.6)	99.1 (53.0)
R _{merge} [†]	0.218 (0.989)	0.193 (1.383)	0.242 (1.325)
<I/σ(I)>	12.0 (2.7)	12.5 (1.8)	9.0 (1.7)
Multiplicity	11.0 (10.9)	11.1 (11.1)	11.0 (10.8)
Wilson B factor (Å ⁻²)	19.95	16.80	8.14
Refinement			
Reflections used	35215 (2533)	69572 (5027)	80956 (5879)
Reflections used for R _{free}	1850 (150)	3505 (254)	4196 (293)
R factor [‡] (%)	19.5 (26.4)	18.1 (28.7)	18.4 (28.7)
R _{free} [‡] (%)	25.2 (32.4)	21.5 (32.0)	22.2 (30.4)
R.m.s.d. bond lengths (Å)	0.013	0.009	0.019
R.m.s.d. bond angles (°)	1.650	1.466	1.712
R.m.s.d. chirals (Å ³)	0.101	0.085	0.113
No. of non-H atoms (total)	5736	6042	6324
No. of water molecules	238	441	700
No. of ligand atoms	165	241	216
No. of ions	3	1	9
Mean B factor (Å ²)			
Non-H atoms	25.04	21.20	13.17
Water molecules	22.99	28.32	20.72
Ligands	39.12	35.44	24.64
Ions	32.40	36.76	23.78
Ramachandran plot (%)			
Residues in most favourable regions	95.8	97.2	96.7
Residues in allowed regions	4.2	2.8	3.3
Rotamer outliers (%)	3.2	3.2	3.5

Table 5. Data collection and refinement statistics for PHL complexes. Values in parentheses correspond to the highest resolution shell. [†]R_{merge} = $\sum |I_i - \langle I \rangle| / \sum I_i$, where I_i is the intensity of observation and $\langle I \rangle$ is the mean value for that reflection. [‡]R factor = $\sum | |F_o(h)| - |F_c(h)| | / \sum_h F_o(h)$, where F_o and F_c are the observed and calculated structure-factor amplitudes, respectively.

further supporting the previously reported presence of lectins on surface as was also proved for other bacteria (e.g. *P. aeruginosa*, *E. coli*)^{31,33–35}.

Based on the findings presented in this work, we consider these compounds as a milestone on the way to design efficient inhibitors targeting *P. asymbiotica*.

Methods

Ligand preparation. All ligands were prepared as 50 mM stock solutions. Lyophilized azide 1, fucosides 2–4, difucoside 5, and dendrimers 8–10 were dissolved in the deionized water, whereas calixarenes 6–7 were dissolved in DMSO.

Protein production and purification. The PHL lectin was produced in *Escherichia coli* Tuner(DE3)/pET25b_phl cells as previously published¹⁶. In short, the cells were grown in LB broth medium containing 100 μM ampicillin at 37 °C. After reaching an OD₆₀₀ of 0.5, gene expression was induced with 0.2 mM isopropyl

Molecule	PHL/fucoside 2		PHL/fucoside 3		PHL/fucoside 4	
	A	B	A	B	A	B
Site 1	FA	FA	FA	FA	FA	FA
Site 2	Met60	Met60	Met60	Met60	Met60	Met60
Site 3	FA	FA	FA	FA	FA	FA
Site 4	F	F	FA	FA	FA	F
Site 5	—	FA	F	FA	FA	F
Site 6	F	F	FA	FA	F	FA
Site 7	F	F	FA	FA	F	FA

Table 6. Binding site occupancy of PHL complexes with fucosides 2–4. F – fucosyl moiety, A – D-arabino-hexopyranosyl moiety, Met60 – Met60 from symmetry-related PHL molecule.

β -D-1-thiogalactopyranoside (IPTG). Cells were incubated for an additional 20 hours at 18 °C, harvested by centrifugation at 12,000 g for 10 min and resuspended in buffer A (20 mM Tris/HCl, 300 mM NaCl, pH 7.5). Harvested cells were stored at –20 °C prior to protein purification.

For protein purification, cells were disintegrated by sonication (VCX 500, Sonics & Materials, Inc., USA) and the cytosolic fraction containing soluble PHL was collected by centrifugation at 21,000 g at 4 °C for 1 hour and filtrated through a 0.45 μ m pore size filter (Carl Roth, Germany). Recombinant protein PHL was purified with isocratic elution on a D-mannose-agarose (Sigma-Aldrich, USA) resin equilibrated with buffer A by affinity chromatography using an ÄKTA FPLC system (GE Healthcare, UK) and used for further studies. For agglutination assays, purified PHL was dialyzed against PBS buffer (137 mM NaCl, 2.7 mM KCl, 8 mM Na₂HPO₄, 1.47 mM KH₂PO₄, pH 7.4).

Hemagglutination inhibition assay. Human red blood cells (RBCs) O were processed according to previously published work¹⁶. In brief, RBCs O treated with sodium citrate were washed four times by PBS buffer (137 mM NaCl, 2.7 mM KCl, 8 mM Na₂HPO₄, 1.47 mM KH₂PO₄, pH 7.4), diluted to 50% by PBS with 0.005% (w/w) sodium azide and treated by 0.1% papain for the duration of 30 minutes.

Hemagglutination inhibition assay was performed for specificity and semi-quantitative affinity of the PHL interaction with the compounds. All carbohydrate inhibitors in 50 mM starting concentration were serially diluted in the PBS buffer and used for a determination of the lowest inhibiting concentration. As a blank, the PBS buffer supplemented with the appropriate amount of DMSO was used in order to exclude potential interference with the interaction. The individual samples were mixed with the lectin in concentration 2 mg/ml in a 5 μ l:5 μ l ratio. Thereafter, 10 μ l of 10% RBCs O in PBS buffer was added, thoroughly mixed and incubated for 10 minutes at room temperature³⁶. Following incubation, the mixture was again mixed and the reaction was observed on microscope slides using Levenhuk 2L NG microscope with Levenhuk D2L digital camera (Levenhuk, USA). Images were obtained via software ToupView for Windows (Levenhuk). The positive (PHL without inhibitor) and negative control (reaction without PHL) were prepared and processed in the same way using the appropriate volume of PBS buffer instead of the not included components. The lowest concentration of inhibitor able to inhibit agglutination was determined and compared with the standard (L-fucose). Minimal inhibitory concentrations (MIC) of synthesised inhibitors were determined from two independent measurements.

Surface plasmon resonance. Surface plasmon resonance (SPR) experiments were performed on a BIAcore T200 instrument (GE Healthcare, UK) at 25 °C, using buffer A supplemented with 0.05% Tween 20 as a running buffer. α -L-fucoside was immobilized onto CM5 sensor chip (GE Healthcare, UK) covered with a carboxymethylated dextran matrix. The sensor chip surface was activated with N-ethyl-N-(3-dimethylaminopropyl)carbodiimide/N-hydroxysuccinimide solution and then coated with streptavidin using the manufacturer's standard protocol using HBS buffer (10 mM HEPES, 150 mM NaCl, 0.05% Tween 20, pH 7.5). Unreacted groups were blocked with 1 M ethanolamine-HCl, pH 8.5. Biotinylated carbohydrate (biotinylated monomeric probes, Lectinity, Russia) was injected onto particular measuring channel and pure biotin on blank channel at a flow rate of 5 μ l/min.

SPR inhibition measurements were carried out on measuring channel with L-fucoside at a flow rate of 5 μ l/min. PHL was diluted to a concentration of 20 μ g/ml by the buffer A supplemented with 0.05% Tween 20, mixed 1:1 (v/v) with various concentrations of inhibitors (500–5 μ M) in the same buffer and injected onto the sensor chip. The response of lectin bound to the sugar surface at equilibrium was plotted against the concentration of inhibitor in order to determine IC₅₀ (concentration of inhibitor resulting in 50% inhibition of binding). As IC₅₀ is not a constant and depends on the experimental set-up, a parameter called potency was used for characterization. The potency of a tested inhibitor is the ratio of IC₅₀ of a chosen standard inhibitor (in this case L-fucose) and the inhibitor in question. Pure PHL lectin was used as a control (0% inhibition) and channel with pure biotin served as a blank. IC₅₀ was determined from triplicates.

Isothermal titration calorimetry. PHL protein in buffer A was equilibrated at room temperature at least for 30 min before ITC measurement. All ITC experiments were performed using ITC200 calorimeter (Malvern Panalytical, UK) at 25 °C. Carbohydrate ligands dissolved in buffer A were used at different concentrations. Protein in the calorimeter cell (50 μ M) was titrated by consecutive additions (2 μ l) of the ligand (1.5–5 mM) in the syringe while stirring at 1000 rpm. Integrated heat effects were analysed by nonlinear regression using a single-site binding model and global fitting in Origin 7 software (Microcal Instruments)³⁷. The thermodynamic parameters of synthesised inhibitors were determined from two independent measurements.

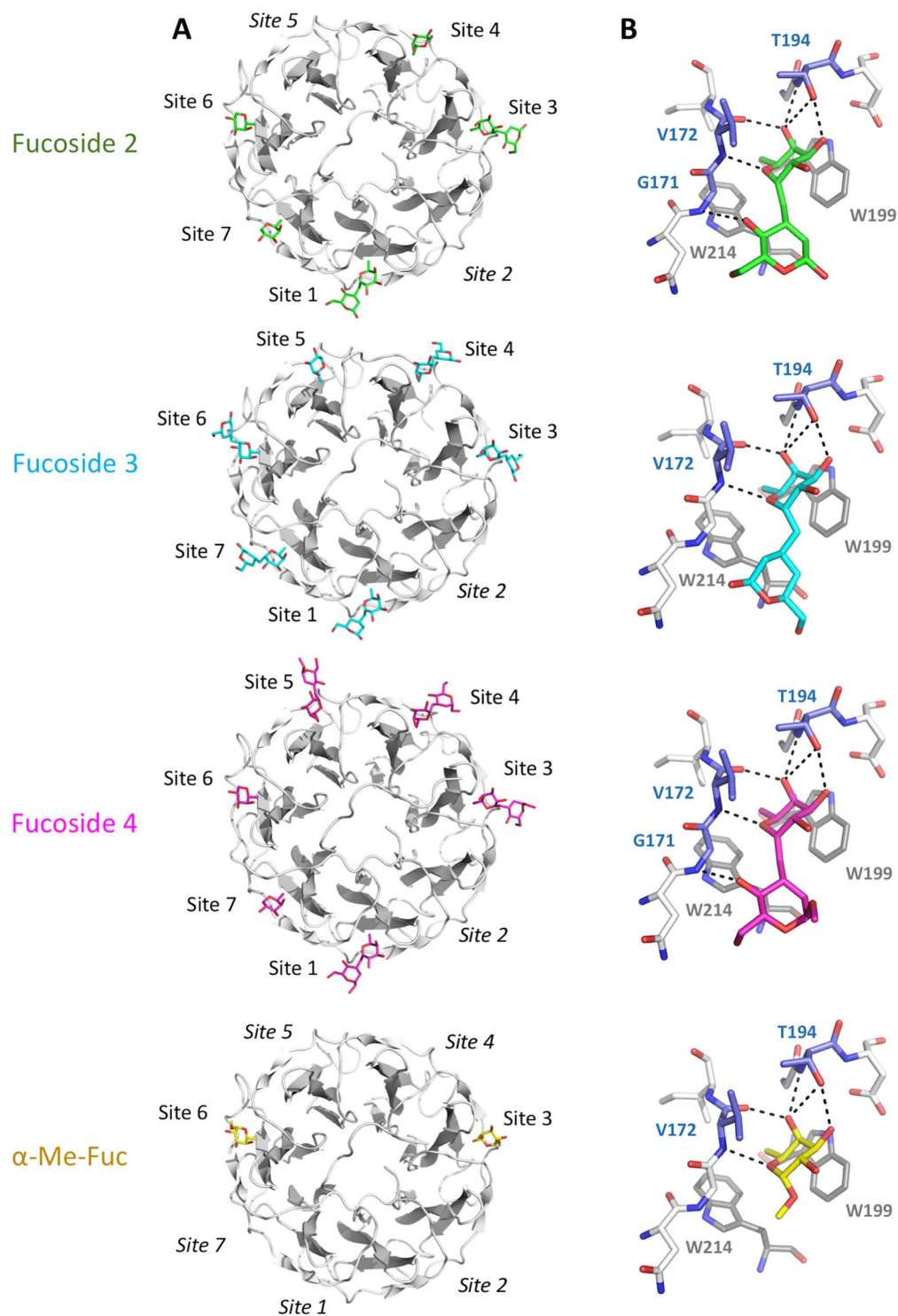


Figure 6. Structure of PHL with fucosides 2–4 and α -Me-Fuc from 5MXE structure for comparison. **(A)** Overall structure of chain A of PHL complexes. Individual binding sites labelled, label in italics for empty site. Fucosides shown as sticks. **(B)** Binding site 3 with coordinated ligand. Key residues labelled. Colour code: fucoside 2 – green, fucoside 3 – cyan, fucoside 4 – magenta, α -Me-Fuc – yellow, CH- π interacting tryptophans – grey, H-bond interacting residues – blue.

Crystallization and data collection. PHL was concentrated to 13.6 mg/ml using an ultrafiltration unit with a 10-kDa cut-off membrane (Vivaspin 20, Sartorius, Germany) and crystallized under previously described conditions¹⁶. The crystals were obtained under the following conditions: 4 μ l sitting drop, protein solution mixed with precipitant (3.7 M NaCl, 100 mM Hepes, pH 7.5) in ratios 1:1, 3:5, 1:3 and 1:7. The drops were set against

0.5 ml of the same equilibration precipitant. To determine the PHL structure complexed with fucosides 2–4, the crystals of PHL were soaked in a 10 mM solution of compounds 2–4 for 1 hour. The crystals were cryo-protected using 40% PEG 400 and frozen in liquid nitrogen. The diffraction data of PHL complexed with saccharides were collected at the BESSY II electron storage ring (Berlin-Adlershof, Germany)³⁸.

Structure determination. Images were processed using XDSAPP³⁹ and converted to structure factors using the program package CCP4 v.6.5⁴⁰, with 5% of the data reserved for R_{free} calculation. The structures of PHL complexes were solved by molecular replacement with Phaser⁴¹ using the monomeric coordinates of the ligand-free PHL structure (5MXE). Refinement of the molecule was performed using REFMAC5⁴² alternated with manual model building in Coot v.0.8⁴³. Sugar-derived ligand coordinates were established using JLigand⁴⁴ included in CCP4 program package. Ligands and other compounds that were present were placed manually using Coot. Water molecules were added by Coot and checked manually. The addition of alternative conformations, where necessary, resulted in final structures that were validated using the MolProbity⁴⁵ (<http://molprobity.biochem.duke.edu>) validation server and were deposited in the PDB as entries 6FHX, 6FHY and 6FLU. Molecular drawings were prepared using Pymol (Schrödinger, Inc.).

P. asymbiotica growth. *P. asymbiotica* subsp. *australis* was inoculated from stock cells stored at -80°C into a standard LB media and were grown in 30°C under an orbital shaking overnight. Bacterial growth was tracked by measuring the optical density of the broth at 600 nm (OD_{600}) using a spectrophotometer (Biochrom Ltd., BioPhotometer WGA CO 8000 Biowave). Cells were harvested when reaching an $\text{OD}_{600} = 0.5$. The culture was centrifuged at 4,300 g and room temperature for 2 minutes (Minispin, Eppendorf, Germany) and cells were then washed three times with PBS buffer. Cells were diluted in PBS to OD_{600} of 2.0 and kept in a fridge until performing the aggregation assay.

Cell aggregation assay. *P. asymbiotica* subsp. *australis* cells and fucosylated compounds in a concentration ranging from 50 mM to 3.125 mM were gently mixed in a 9:1 (v/v) ratio. The reaction mixtures were left at room temperature for 10 minutes. 5 μl of reaction mixture was then transferred onto a microscope slide and observed under a fluorescence microscope (OLYMPUS IX81 Microscope IX81F-3 with IX2-UCB-2 Controller and X-Cite 120PC Q; Olympus and Excelitas Technologies, Japan, resp. USA). As a negative control, bacterial cells with/without azide 1 as a monomer were used. Three independent measurements were performed.

Received: 23 March 2018; Accepted: 30 September 2019;

Published online: 17 October 2019

References

- Varki, A. Biological roles of glycans. *Glycobiology* **27**, 3–49 (2017).
- Sharon, N. Carbohydrates as future anti-adhesion drugs for infectious diseases. *Biochim. Biophys. Acta* **1760**, 527–537 (2006).
- Imberty, A., Wimmerová, M., Mitchell, E. P. & Gilboa-Garber, N. Structures of the lectins from *Pseudomonas aeruginosa*: insight into the molecular basis for host glycan recognition. *Microbes Infect.* **6**, 221–228 (2004).
- Farmer, J. J. *et al.* *Xenorhabdus luminescens* (DNA hybridization group 5) from human clinical specimens. *J. Clin. Microbiol.* **27**, 1594–1600 (1989).
- Peel, M. M. *et al.* Isolation, identification, and molecular characterization of strains of *Photorhabdus luminescens* from infected humans in Australia. *J. Clin. Microbiol.* **37**, 3647–3653 (1999).
- Mulley, G. *et al.* From insect to man: *Photorhabdus* sheds light on the emergence of human pathogenicity. *PLoS One* **10**, e0144937 (2015).
- Gerrard, J. G. *et al.* Nematode symbiont for *Photorhabdus asymbiotica*. *Emerg. Infect. Dis.* **12**, 1562–1564 (2006).
- Peat, S. M. *et al.* A robust phylogenetic framework for the bacterial genus *Photorhabdus* and its use in studying the evolution and maintenance of bioluminescence: A case for 16S, gyrB, and glnA. *Mol. Phylogenet. Evol.* **57**, 728–740 (2010).
- Kuwata, R., Yoshiga, T., Yoshida, M. & Kondo, E. Mutualistic association of *Photorhabdus asymbiotica* with Japanese heterorhabditid entomopathogenic nematodes. *Microbes Infect.* **10**, 734–741 (2008).
- Thanwisai, A. *et al.* Diversity of *Xenorhabdus* and *Photorhabdus* spp. and their symbiotic entomopathogenic nematodes from Thailand. *PLoS ONE* **7**, e43835 (2012).
- Gerrard, J. G., McNeven, S., Alfredson, D., Forgan-Smith, R. & Fraser, N. *Photorhabdus* species: bioluminescent bacteria as emerging human pathogens? *Emerg. Infect. Dis.* **9**, 251–254 (2003).
- Gerrard, J., Waterfield, N., Vohra, R. & French-Constant, R. Human infection with *Photorhabdus asymbiotica*: an emerging bacterial pathogen. *Microbes Infect.* **6**, 229–237 (2004).
- Weissfeld, A. S. *et al.* *Photorhabdus asymbiotica*, a pathogen emerging on two continents that proves that there is no substitute for a well-trained clinical microbiologist. *J. Clin. Microbiol.* **43**, 4152–4155 (2005).
- Costa, S. C. P. *et al.* Recent insight into the pathogenicity mechanisms of the emergent pathogen *Photorhabdus asymbiotica*. *Microbes Infect.* **12**, 182–189 (2010).
- Machado, R. A. R. *et al.* Whole-genome-based revisit of *Photorhabdus* phylogeny: proposal for the elevation of most *Photorhabdus* subspecies to the species level and description of one novel species *Photorhabdus bodei* sp. nov., and one novel subspecies *Photorhabdus laumondii* subsp. *clarkei* subsp. nov. *Int. J. Syst. Evol. Microbiol.* **68**, 2664–2681 (2018).
- Jančáříková, G. *et al.* Characterization of novel bangle lectin from *Photorhabdus asymbiotica* with dual sugar-binding specificity and its effect on host immunity. *PLOS Pathog.* **13**, e1006564 (2017).
- Chemani, C. *et al.* Role of LecA and LecB lectins in *Pseudomonas aeruginosa* - induced lung injury and effect of carbohydrate ligands. *Infect. Immun.* **77**, 2065–2075 (2009).
- Wu, X. R., Sun, T. T. & Medina, J. J. *In vitro* binding of type 1-fimbriated *Escherichia coli* to uroplakins Ia and Ib: relation to urinary tract infections. *Proc. Natl. Acad. Sci. USA* **93**, 9630–9635 (1996).
- Kumar, A. *et al.* A novel fucose-binding lectin from *Photorhabdus luminescens* (PLL) with an unusual hepta-bladed β -propeller tetrameric structure. *J. Biol. Chem.* **291**, 25032–25049 (2016).
- Beshr, G. *et al.* *Photorhabdus luminescens* lectin A (PLLA): A new probe for detecting α -galactoside-terminating glycoconjugates. *J. Biol. Chem.* **292**, 19935–19951 (2017).
- Diggle, S. P. *et al.* The galactophilic lectin, LecA, contributes to biofilm development in *Pseudomonas aeruginosa*. *Environ. Microbiol.* **8**, 1095–1104 (2006).
- Bertolotti, B. *et al.* Polyvalent C-glycomimetics based on l-fucose or d-mannose as potent DC-SIGN antagonists. *Org. Biomol. Chem.* **15**, 3995–4004 (2017).

23. Bertolotti, B. *et al.* Nonhydrolyzable C-disaccharides, a new class of DC-SIGN ligands. *Carbohydr. Res.* **435**, 7–18 (2016).
24. Kašáková, M. *et al.* Selectivity of original C-hexopyranosyl calix[4]arene conjugates towards lectins of different origin. *Carbohydr. Res.* **469**, 60–72 (2018).
25. Rostovtsev, V. V., Green, L. G., Fokin, V. V. & Sharpless, K. B. A Stepwise Huisgen Cycloaddition Process: Copper(I)-Catalyzed Regioselective “Ligation” of Azides and Terminal Alkynes. *Angew. Chem. Int. Ed.* **41**, 2596–2599 (2002).
26. Tornøe, C. W., Christensen, C. & Meldal, M. Peptidotriazoles on Solid Phase: [1,2,3]-Triazoles by Regiospecific Copper(I)-Catalyzed 1,3-Dipolar Cycloadditions of Terminal Alkynes to Azides. *J. Org. Chem.* **67**, 3057–3064 (2002).
27. Lundquist, J. J. & Toone, E. J. The cluster glycoside effect. *Chem. Rev.* **102**, 555–578 (2002).
28. Cecioni, S., Imberty, A. & Vidal, S. Glycomimetics versus multivalent glycoconjugates for the design of high affinity lectin ligands. *Chem. Rev.* **115**, 525–561 (2015).
29. Bernardi, A. *et al.* Multivalent glycoconjugates as anti-pathogenic agents. *Chem. Soc. Rev.* **42**, 4709–4727 (2013).
30. Tabarani, G. *et al.* DC-SIGN neck domain is a pH-sensor controlling oligomerization: SAXS and hydrodynamic studies of extracellular domain. *J. Biol. Chem.* **284**, 21229–21240 (2009).
31. Jančáříková, G. *et al.* Synthesis of α -L-fucopyranoside-presenting glycoclusters and investigation of their interaction with recombinant *Photobacterium aeruginosa* lectin (PHL). *Chem. - Eur. J.*, <https://doi.org/10.1002/chem.201705853> (2018).
32. Mitchell, E. P. *et al.* High affinity fucose binding of *Pseudomonas aeruginosa* lectin PA-III: 1.0 Å resolution crystal structure of the complex combined with thermodynamics and computational chemistry approaches. *Proteins Struct. Funct. Bioinforma.* **58**, 735–746 (2004).
33. Boukerb, A. M. *et al.* Antiadhesive properties of glycoclusters against *Pseudomonas aeruginosa* lung infection. *J. Med. Chem.* **57**, 10275–10289 (2014).
34. Yu, G. *et al.* A Sugar-functionalized amphiphilic pillar[5]arene: Synthesis, self-assembly in water, and application in bacterial cell agglutination. *J. Am. Chem. Soc.* **135**, 10310–10313 (2013).
35. Gestwicki, J. E., Strong, L. E., Cairo, C. W., Boehm, F. J. & Kiessling, L. L. Cell aggregation by scaffolded receptor clusters. *Chem. Biol.* **9**, 163–169 (2002).
36. Adamová, L., Malinová, L. & Wimmerová, M. New sensitive detection method for lectin hemagglutination using microscopy. *Microsc. Res. Tech.* **77**, 841–849 (2014).
37. Wiseman, T., Williston, S., Brandts, J. F. & Lin, L.-N. Rapid measurement of binding constants and heats of binding using a new titration calorimeter. *Anal. Biochem.* **179**, 131–137 (1989).
38. Mueller, U. *et al.* Facilities for macromolecular crystallography at the Helmholtz-Zentrum Berlin. *J. Synchrotron Radiat.* **19**, 442–449 (2012).
39. Krug, M., Weiss, M. S., Heinemann, U. & Mueller, U. XDSAPP: a graphical user interface for the convenient processing of diffraction data using XDS. *J. Appl. Crystallogr.* **45**, 568–572 (2012).
40. Winn, M. D. *et al.* Overview of the CCP 4 suite and current developments. *Acta Crystallogr. D Biol. Crystallogr.* **67**, 235–242 (2011).
41. McCoy, A. J. *et al.* Phaser crystallographic software. *J. Appl. Crystallogr.* **40**, 658–674 (2007).
42. Murshudov, G. N. *et al.* REFMAC 5 for the refinement of macromolecular crystal structures. *Acta Crystallogr. D Biol. Crystallogr.* **67**, 355–367 (2011).
43. Emsley, P., Lohkamp, B., Scott, W. G. & Cowtan, K. Features and development of Coot. *Acta Crystallogr. D Biol. Crystallogr.* **66**, 486–501 (2010).
44. Lebedev, A. A. *et al.* JLigand: a graphical tool for the CCP4 template-restraint library. *Acta Crystallogr. D Biol. Crystallogr.* **68**, 431–440 (2012).
45. Chen, V. B. *et al.* MolProbity: all-atom structure validation for macromolecular crystallography. *Acta Crystallogr. D Biol. Crystallogr.* **66**, 12–21 (2010).

Acknowledgements

The project was supported by the Czech Science Foundation (15-17572S, 18-18964S). We acknowledge the Biomolecular Interactions and Crystallization Core Facility of CEITEC supported by the CIISB research infrastructure (LM2015043) funded by MEYS CR for their support with obtaining scientific data presented in this paper. Diffraction data have been collected on BL14.3 at the BESSY II electron storage ring operated by the Helmholtz-Zentrum Berlin (Mueller *et al.*, 2015). We would particularly like to acknowledge the help and support of Franziska Huschmann during the experiment. The funders had no role in study design, data collection and analysis, decision to publish, or preparation of the manuscript. We also thank Ben Watson-Jones for language corrections.

Author contributions

M.W. and J.M. designed the study. M.K., B.B., B.O. synthesized the fucosylated ligands, G.J. and J.H. conducted experiments. J.M., K.P. and M.W. supervised experiments and validated the results. G.J., J.H., J.M. and M.W. wrote the paper.

Competing interests

The authors declare no competing interests.

Additional information

Correspondence and requests for materials should be addressed to M.W.

Reprints and permissions information is available at www.nature.com/reprints.

Publisher's note Springer Nature remains neutral with regard to jurisdictional claims in published maps and institutional affiliations.



Open Access This article is licensed under a Creative Commons Attribution 4.0 International License, which permits use, sharing, adaptation, distribution and reproduction in any medium or format, as long as you give appropriate credit to the original author(s) and the source, provide a link to the Creative Commons license, and indicate if changes were made. The images or other third party material in this article are included in the article's Creative Commons license, unless indicated otherwise in a credit line to the material. If material is not included in the article's Creative Commons license and your intended use is not permitted by statutory regulation or exceeds the permitted use, you will need to obtain permission directly from the copyright holder. To view a copy of this license, visit <http://creativecommons.org/licenses/by/4.0/>.

© The Author(s) 2019